

# Interactions of Granisetron with an Agonist-Free 5-HT<sub>3A</sub> Receptor Model

Prasad R. Joshi,<sup>‡,§</sup> Asha Suryanarayanan,<sup>‡,§</sup> Eszter Hazai,<sup>||</sup> Marvin K. Schulte,<sup>§</sup> Gábor Maksay,<sup>||</sup> and Zsolt Bikádi<sup>\*,||</sup>

Department of Chemistry and Biochemistry, The University of Alaska, Fairbanks, Alaska 99775, and Department of Molecular Pharmacology, Institute of Biomolecular Chemistry, Chemical Research Center, Budapest, Post Office Box 17, H-1525, Hungary

Received August 23, 2005; Revised Manuscript Received December 5, 2005

**ABSTRACT:** A new homology model of type-3A serotonin receptors (5-HT<sub>3A</sub>Rs) was built on the basis of the electron microscopic structure of the nicotinic acetylcholine receptor and with an agonist-free binding cavity. The new model was used to re-evaluate the interactions of granisetron, a 5-HT<sub>3A</sub>R antagonist. Docking of granisetron identified two possible binding modes, including a newly identified region for antagonists formed by loop B, C, and E residues. Amino acid residues L184–D189 in loop B were mutated to alanine, while Y143 and Y153 in loop E were mutated to phenylalanine. Mutation H185A resulted in no detectable granisetron binding, while D189A resulted in a 22-fold reduction in affinity. Y143F and Y153F decreased granisetron affinity to the same extent as Y143A and Y153A mutations, supporting the role of the OH groups of these tyrosines in loop E. Modeling and mutation studies suggest that granisetron plays its antagonist role by hindering the closure of the back wall of the binding cavity.

The 5-hydroxytryptamine type-3 receptor (5-HT<sub>3</sub>R) is one of the earliest identified receptors for serotonin (1) and is a member of the Cys-loop ligand-gated ion channel (LGIC) family that includes nicotinic acetylcholine (nACh), glycine, and GABA<sub>A</sub> receptors (2). 5-HT<sub>3</sub>Rs form pentamers (3, 4). Each subunit has an extracellular N-terminal domain and a transmembrane domain consisting of four membrane-spanning segments. A subunits form homopentamers, heteromers with B subunits, and function as nonselective cation channels. In the central nervous system, 5-HT<sub>3</sub>Rs are mainly found as homomeric 5-HT<sub>3A</sub>Rs (5). The functional role of human genes of 5-HT<sub>3</sub>R C, D, and E subunits (6) is not known.

Proteins of biological interest can be studied at the atomic level after their structure has been determined by X-ray crystallography. However, the structure of the 5-HT<sub>3</sub> receptor has not yet been determined. The determination of the X-ray structure of an acetylcholine-binding protein (AChBP) from *Lymnaea stagnalis* (7) (sharing about 20% sequence identity with the extracellular domain of the 5-HT<sub>3</sub> receptor) has greatly contributed to our understanding of the function and structure of LGICs. Modeling studies have utilized this structural information from the snail AChBP in the analysis of receptor–ligand interactions. Homology modeling of the 5-HT<sub>3</sub> receptor based on this structure has provided information about the molecular basis of ligand–receptor interactions (8–11). The effects of individual residues on ligand binding have been tested by site-directed mutagenesis (11–19). Recently, an inhibitor-bound AChBP from *Aplysia californica* has been crystallized (20), revealing significant differ-

ences in the agonist- (21) and inhibitor-bound conformations of the receptors. Further, the electron microscopic structure of the nACh receptor has been refined at 4 Å resolution (22). The nACh receptor, with a considerably closer structural relationship with the 5-HT<sub>3</sub>R, is more suitable as a template for homology modeling studies of members of the LGIC superfamily such as 5-HT<sub>3</sub>Rs because they have closer structural and functional relationships. A consensus seems to be emerging that the acetylcholine-binding site contacts around a bound agonist and less so around a bound antagonist, similar to what occurs with other members of the LGIC superfamily, including AMPA-type glutamate receptors. Loop C of the Cys-loop LGIC family serves as a “lid” on the binding site cavity, and the “lid-shut” conformation seems to correspond to the activated ionophore (23). Accordingly, a ligand-free, “lid-open” ionophore might be a better template to study interactions with antagonists than the “lid-shut” state.

In the current study, we show the first homology model of the 5-HT<sub>3</sub>R constructed using the experimentally determined ligand-free (closed-channel) structure of the nACh receptor–ionophore. The docking of granisetron to the binding pocket suggests a putative “way-in site” of interaction of granisetron with the 5-HT<sub>3A</sub>R. To provide experimental evidence for this model, mutation studies were carried out to test the involvement of individual residues. Mutational studies support our model, predicting a “way-in site” of interaction of granisetron with 5-HT<sub>3A</sub>Rs.

## EXPERIMENTAL PROCEDURES

*Xenopus laevis* frogs and frog food were purchased from Xenopus Express (Homosassa, FL). Sigma type-II collagenase was purchased from Sigma–Aldrich (St. Louis, MO). [<sup>3</sup>H]Granisetron was purchased from New England Nuclear (Brattleboro, VT). All other chemicals were obtained from Fisher Scientific (Houston, TX).

\* To whom correspondence should be addressed: Zsolt Bikádi Department of Molecular Pharmacology, Institute of Biomolecular Chemistry, Chemical Research Center, Budapest, Post Office Box 17, H-1525, Hungary. Telephone: (361) 3257900. Fax: (361) 3257554. E-mail: bikadi@chemres.hu.

† These two authors contributed equally to the following work.

§ The University of Alaska.

|| Chemical Research Center.

**Cell Culture and Transient Transfections.** *t*SA201 cells (a derivative of HEK 293 cells) were cultured in Dulbecco's modified Eagle medium (DMEM, New Life Technologies, New York) supplemented with 10% fetal bovine serum and 100 units (mL of penicillin)<sup>-1</sup> streptomycin<sup>-1</sup> in a humidified 5% CO<sub>2</sub> atmosphere at 37 °C. For each radioligand-binding study, *t*SA201 cells were plated on 100 mm culture dishes at a density of  $5 \times 10^6$  cells/dish and grown for 9 h prior to transfection. The same number of cells were plated for each experiment. Cells were transfected with 20  $\mu$ g/dish wild-type (wt) or mutant plasmid cDNA using a calcium phosphate transfection kit (New Life Technologies, New York). Transfected cells were supplemented with fresh DMEM 12–15 h later and harvested 48 h after transfection.

**Site-Directed Mutagenesis.** Mouse wt 5-HT<sub>3A</sub>S receptor cDNA was derived from N1E-115 neuroblastoma cells as previously described (15). All mutant receptors were constructed using the pAlter altered sites mutagenesis kit (Promega, San Luis Obispo, CA) and confirmed by restriction digests and DNA sequencing (UC Davis, CA).

**Radioligand-Binding Assays.** Radioligand-binding assays were performed as described earlier (16). Transfected cells were scraped from dishes, washed twice with phosphate-buffered saline (PBS) (New Life Technologies, New York), and then resuspended in 1.0 mL of PBS containing Complete protease inhibitor cocktail in a 100 mm dish (Roche, Mannheim, Germany). Cells were either used fresh or frozen at this step until needed. Immediately prior to use, cells were homogenized in PBS (with protease inhibitor) using a glass tissue homogenizer and then centrifuged at 35000g for 30 min. Membranes were washed once more with PBS and resuspended in a 1 mL PBS/100 mm dish. The total protein content was determined using the Lowry assay (Sigma Diagnostics, St. Louis, MO). For *K<sub>d</sub>* determinations, aliquots of 50  $\mu$ L of homogenate were incubated at 37 °C for 1 h with varying concentrations of [<sup>3</sup>H]granisetron (typically 0.1–100 nM). Binding was terminated by rapid filtration onto GF/B filters. Specific binding was determined to be the amount of [<sup>3</sup>H]granisetron bound in the presence of a saturating concentration of the competitive antagonist tropisetron (10  $\mu$ M). Mutant receptors were tested identically to wt, although concentrations of [<sup>3</sup>H]granisetron were varied to accommodate differences in *K<sub>d</sub>* values. Typically a range of concentrations from 0.1*K<sub>d</sub>* to 10*K<sub>d</sub>* were utilized for these experiments. Variations in *B<sub>max</sub>* values were observed for mutant receptors (see Table 1). Nonspecific binding increased linearly with the ligand concentration and varied with *B<sub>max</sub>* values. For wt receptors, nonspecific binding was ~16% of the total binding. Nonspecific binding in assays with mutant receptors as a percent of the total binding was as follows: L184A, 4%; H185Y, 36%; T186A, 11%; I187A, 22%; Q188A, 6%; D189A, 55%; I190A, 49%; Y143A, 49%; Y143F, 27%; Y153A, 21%; and Y153F, 18%.

**Data Analysis.** *K<sub>d</sub>* and *B<sub>max</sub>* values were determined by nonlinear curve fitting using GraphPad Prism software (San Diego, CA). The combined data from at least four experiments were fit to the following equation:  $B = B_{\max}[L]^n / ([L]^n + K_d^n)$ , where *B* is bound ligand, *B<sub>max</sub>* is the maximum binding, *L* is the ligand concentration, *K<sub>d</sub>* is the equilibrium dissociation constant, and *n* is the Hill coefficient. Data were compared for significant differences using Student's *t* test. *B<sub>max</sub>* and *K<sub>d</sub>* values are given in Table 1.

**Molecular Modeling.** The extracellular regions of homopentameric murine 5-HT<sub>3A</sub>Rs were built on the basis of the recently published three-dimensional structure of the nACh receptor (PDB entry code 2BG9, 22). The sequence of murine 5-HT<sub>3A</sub>R was taken from Protein Information Resource [accession number NF00512558 (24)]. Multiple sequence alignments were performed by "ClustalW" software using default parameters (25). Homology model building of the extracellular region of murine 5-HT<sub>3A</sub>Rs based on the  $\alpha$  and  $\delta$  subunits of the nACh receptor was carried out using "Nest" (26) and "Loopy" (27) programs of the Jackal protein structure modeling package. Refinements of the resulting structures were carried out by the "Minst" program of Jackal on a Silicon Graphics Octane workstation under Irix 6.5 operation system. The homopentamer was built from "distorted" (homology model of  $\alpha$  subunits) and "non- $\alpha$ -conformation" monomers (homology model of  $\delta$  subunit) and assembled on the basis of the nACh structure, in the order of "lid-open", "lid-shut", "lid-open", "lid-shut", "lid-shut" monomers, to reach a minimal root-mean-square deviation (rmsd) between the matched monomers. Finally, the assembled homopentamer was energy-minimized again using the same parameters, as previously described (8). The quality of the model was verified using Procheck, and more than 99.5% of the dihedral angles were found in the allowed region of the Ramachandran plot (28). Docking calculations were carried out at the interface of the  $\alpha$ -subunit-based ("lid-open") and  $\delta$ -subunit-based ("lid-shut") dimeric part of the pentamer.

AutoDock 3.0 (29) was applied for docking calculations, using the Lamarckian genetic algorithm (LGA) and the pseudo-Solis and Wets (pSW) methods. Gasteiger–Huckel partial charges were applied both for ligands and proteins. Solvation parameters were added to the protein coordinate file, and the ligand torsions were defined using the "Addsol" and "Autotors" utilities, respectively, in Autodock 3.0. The atomic affinity grids were prepared with 0.375 Å spacing using the Autogrid program for a 22.5  $\times$  33.75  $\times$  15 Å box around the interface of subunits. Random starting positions, orientations, and torsions (for flexible bonds) were used for the ligands. Each docking run consisted of 100 cycles. The number of evaluations was set to 1.5 million. Final structures with a rmsd less than 2 Å were considered to belong to the same cluster.

## RESULTS

**Homology Modeling of the "Lid-Open" 5-HT<sub>3A</sub>R.** The recently published structure of the Torpedo nACh receptor (PDB entry code 2BG9, 22) is the first LGIC whose structure has been published. This structure allows us to build a more suitable homology model for 5-HT<sub>3</sub>Rs, capable of better prediction of binding interactions of antagonists with 5-HT<sub>3</sub>-Rs (sequence identities of the murine 5-HT<sub>3A</sub>R  $\alpha$  subunit with  $\alpha$ ,  $\beta$ ,  $\gamma$ , and  $\delta$  subunits of the nACh receptor are 29, 33, 28, and 32%, respectively). Three-dimensional alignment between the AChBP (PDB entry code 1I9B) and nAChR  $\beta$  subunit (PDB entry code 2BG9), sharing only 23% sequence identity, results in a rmsd of backbone atoms as low as 1.26 Å. This level of conservation suggests that homology modeling can reliably predict the three-dimensional structure of 5-HT<sub>3</sub>. More importantly, the ligand-free binding interfaces of the two  $\alpha$  subunits with  $\gamma$  and  $\delta$  subunits in nACh

Table 1: Effects of Amino Acid Mutations of Loop B and E Residues on the  $K_d$  Value of [<sup>3</sup>H]Granisetron Binding (Shaded Rows)<sup>a</sup>

mutation	loop	$K_d$ (nM)	$B_{max}$ (pmol/mg of protein)	fold change in $K_d$	region	A	B
WT		0.96 ± 0.16	12 ± 0.77				
Y73A				not affected (~1) <sup>(17)</sup>	I		+
W90A	D			8.4 <sup>(13)</sup>	I		+
L126	A				I		+
I127	A				I		+
N128A	A			not affected (~1) <sup>(17)</sup>	I		+
E129A	A			no binding <sup>(17)</sup>	I		+
Y141A	E			2.5 <sup>(17)</sup>	III	+	
Y143A	E	3.9 ± 0.42	1.1 ± 0.04	4.1	II	+	+
Y143F	E	3.4 ± 0.31	3.0 ± 0.52	3.5	II	+	+
Y153A	E	6.7 ± 0.7	4.2 ± 0.61	7.0	II	+	+
Y153F	E	6.0 ± 0.3	4.9 ± 0.19	6.3	II	+	+
T181A	B			0.4 <sup>(17)</sup>	I		+
S182A	B			3.2 <sup>(17)</sup>	II	+	+
W183A	B			no binding <sup>(17)</sup>	II	+	+
L184A	B	4.7 ± 0.28	21 ± 1.0	4.9	II	+	+
H185A	B	ND			III	+	
H185Y	B	4.9 ± 0.32	1.9 ± 0.05	5.1	III	+	
T186A	B	2.3 ± 0.34	8.2 ± 1.7	2.4	III	+	
I187A	B	3.4 ± 0.46	3.8 ± 1.1	3.5	III		
Q188A	B	1.4 ± 0.10	12 ± 1.1	1.5	III		
D189A	B	22 ± 0.62	0.87 ± 0.04	23.0	III	+	
D229A	C			8.0 <sup>(19)</sup>	II	+	+
S233A	C			no binding <sup>(19)</sup>	II	+	+
Y234A	C			11.0 <sup>(19)</sup>	II	+	+

<sup>a</sup>  $B_{max}$  and  $K_d$  values represent means ± SEM of four experiments at least. Amino acid residues found within 4 Å in the docked models A and B are indicated by +. The effects of mutations in previous studies on granisetron binding (11, 15, 17, 19) are also indicated. ND indicates that the value could not be determined because no binding was observed.

receptors represent the closed state of the ionophore, which is stabilized by antagonists. This is supported by the recent crystal structure of the AChBP–inhibitor complex (PDB entry code 2BR8, 20). Figure 1 shows a comparison of the new 5-HT<sub>3A</sub>R model based on the  $\alpha\delta$ -subunit dimer of nACh receptors and the model based on AChBP from *Lymnaea stagnalis* (PDB entry code 1I9B, 7). As can be seen on Figure 1, the most significant structural difference can be found at the C loop region, where a 15° anticlockwise rotation can be observed upon agonist binding. A relatively low number of intersubunit interactions can be found in the “lid-open” model of the binding cavity. The following residues are predicted to be involved in intersubunit interactions (within 4 Å distance of residues): R55–Y141, K81–Q211, Q83–Q211, D132–Q157, W183–P155, L184–Y143, and L184–K154. Additionally, the predicted intersubunit hydrogen-bonding network of the ligand-bound ionophore predicted to form via W183, Y234, Y143, and Y153 (8, 10) is not present in the ligand-free model. The significantly different local structures of the “lid-open” and “lid-shut” binding

cavities suggest that modeling based on the nACh receptor enables us to model binding interactions of antagonists more correctly.

**Docking of Granisetron to the Ligand-Free Receptor Model.** Docking studies were carried out by the Autodock program using the box indicated in Figure 2. The box contains the whole subunit interface; therefore, docking is not constrained to the area below loop C. To evaluate the docking results, three regions were defined within the box: residues below loop C form region I (e.g., E129 and W90); residues behind and in loop C form region II (e.g., W183, D229, and Y234); and residues above loop C (e.g., Y141 and D189) form region III. It is important to note that the size of granisetron does not permit interactions with residues in regions I–III simultaneously.

The models fell into four clusters designated A1 (cluster frequency, 7%; docking energy, −8.49 kJ/mol), A2 (61%; −9.14 kJ/mol), B1 (19%; −9.62 kJ/mol), and B2 (7%; −9.18 kJ/mol). Granisetron was docked in two positions, one of which involves region II and region III residues (models A1



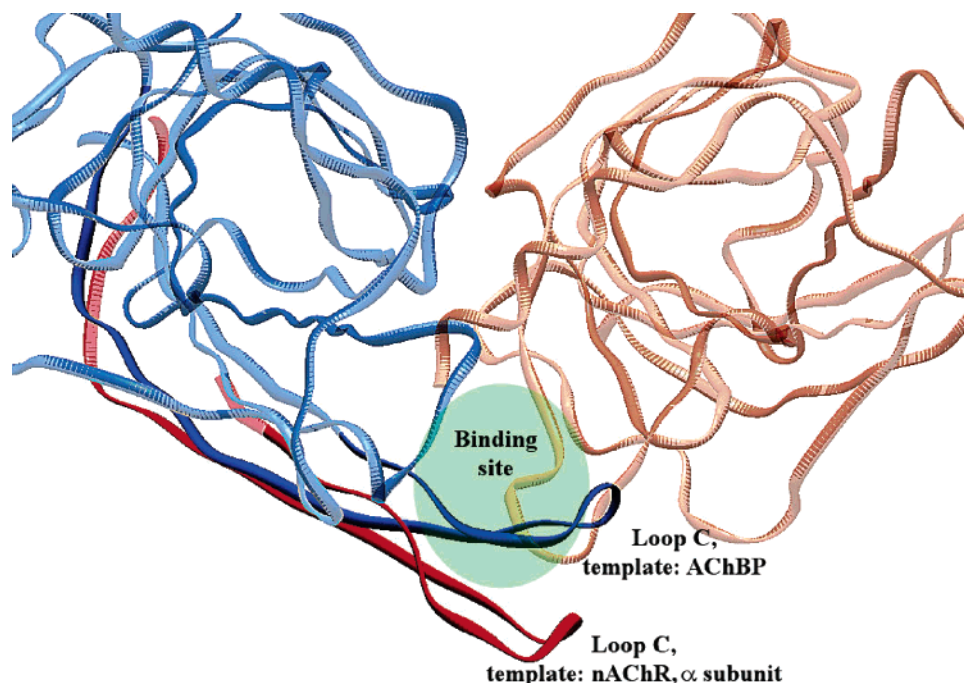


FIGURE 1: Comparison of homology models of the 5HT<sub>3A</sub>R based on AChBP from *Lymnaea stagnalis* (PDB entry code 1I9B) versus the Torpedo nACh receptor (PDB code 2BG9, a subunit). The altered region (loop C, red) of the new model is shown together with the interface region around the binding site of AChBP.

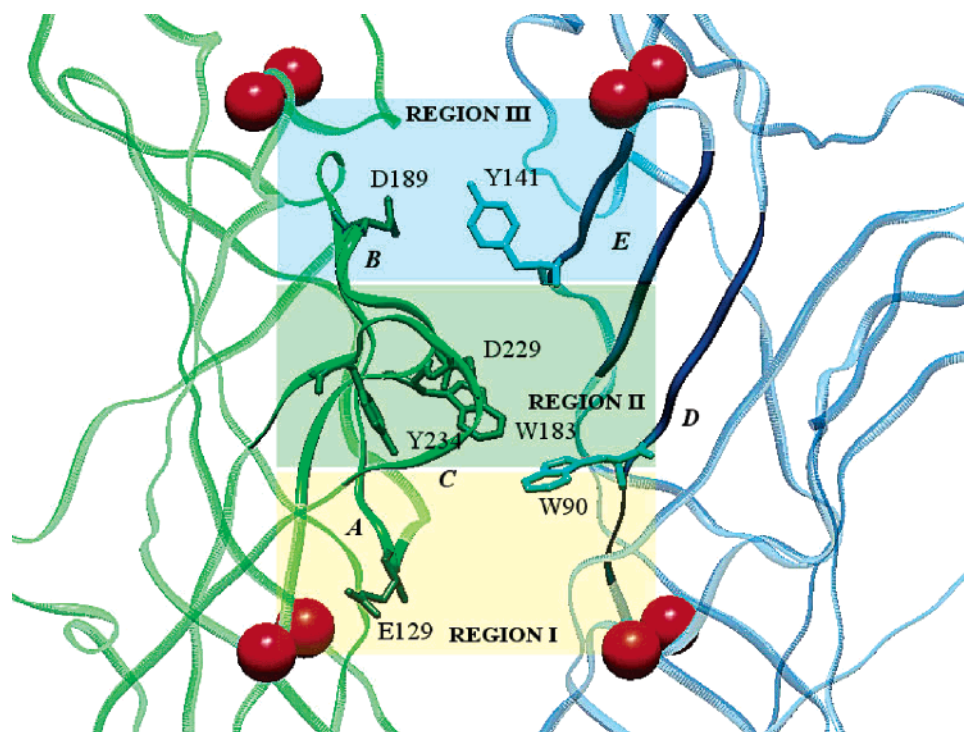


FIGURE 2: Homology model of the 5HT<sub>3A</sub>R based on the nACh receptor. The spheres indicate the edges of the box used in docking studies. Some representative amino acid residues that have been shown experimentally to affect granisetron binding are indicated. Different colors indicate regions I–III for better evaluation of dockings.

and A2, see Figure 3) and the other which involves region I and region II residues (models B1 and B2, see Figure 3). In both positions, granisetron can adopt two orientations: first, where the azobicyclic ring is below loop C (models B1 and A2), and the second, where the aromatic ring occupies the same position (models A1 and B2). Amino acid residues found within 4 Å in the docked models A1 and A2 and models B1 and B2 are summarized in Table 1. The effects of mutations of these residues on granisetron binding

(11, 19) are also indicated. In model A1, granisetron can form the following interactions with the receptor: the ammonium cation of the bicyclic ring can form a salt bridge with the carboxylate anion of D189 or cation- $\pi$  interactions with the aromatic rings of Y141, Y143, and Y153 in loop E and with H185 in loop B. The aromatic ring of granisetron is sufficiently close to W183 and Y234 to form a  $\pi$ - $\pi$  interaction. The carbonyl group can accept a hydrogen bond from Y143 or Y153. In model B1, the ammonium cation

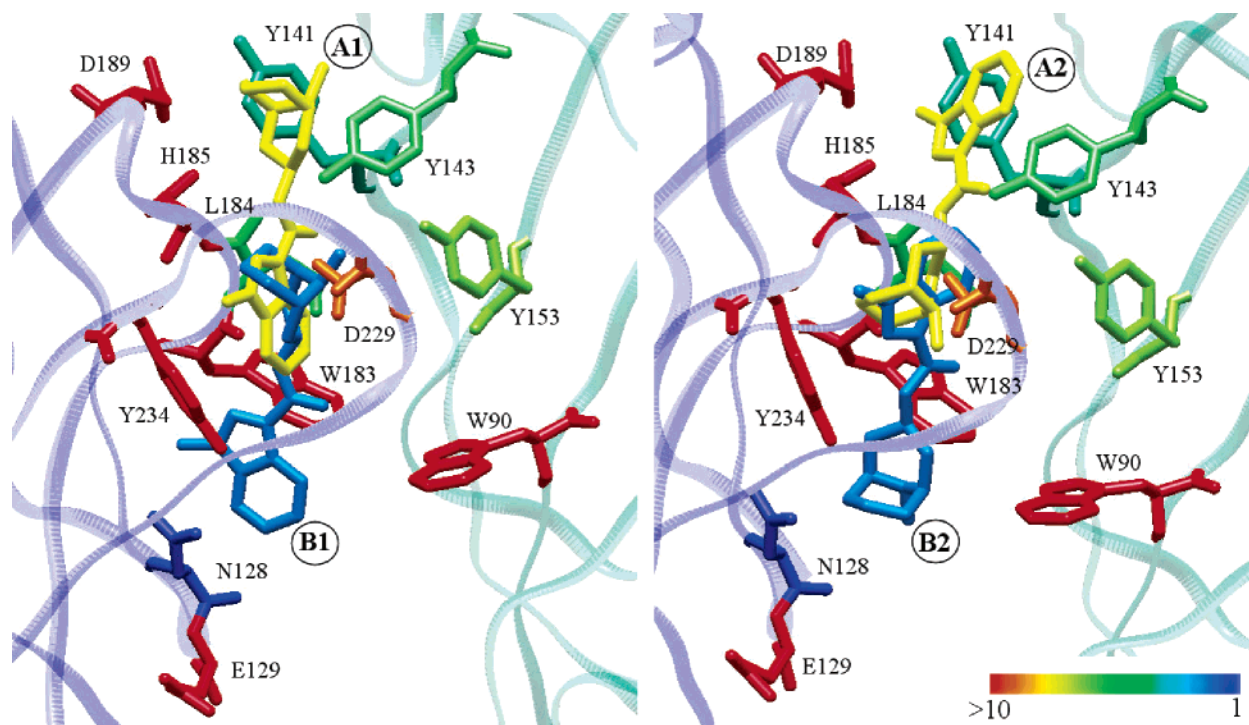


FIGURE 3: Most frequent docking results for granisetron. (Left) Docking location of granisetron in models A1 (yellow) and B1 (blue). Possible hydrogen bondings are indicated by dotted lines. (Right) Models A2 (yellow) and B2 (blue) can be found in the same locations as models A1 and B1, respectively, but in the opposite orientation. The amino acid residues are colored by a temperature factor being proportional to the effect of the alanine mutation on the  $K_d$  value of granisetron binding (see the color bar).

can be salt-bridged with D229 or form cation- $\pi$  interactions with W183, Y234, and Y153. The carbonyl group of granisetron can accept a hydrogen bond from Y234. The aromatic ring is close to W90 in loop D and could interact with N128 and E129. In the reversed orientation (A2 and B2), the same amino acid residues can be involved in the interaction with granisetron. In model A2, the bicyclic ring of granisetron can form a salt bridge with D229, while cation- $\pi$  interactions can be formed with the aromatic residues of region II. The bicyclic ring in this orientation is sufficiently close to W183 to form a cation- $\pi$  interaction. The planar aromatic ring can interact with D189 and Y141. The carbonyl group of granisetron could possibly form a hydrogen bond with Y143 or Y153. In model B2, the bicyclic ring of granisetron is close to W90 and the indole ring can form  $\pi$ - $\pi$  interactions with W183 and Y234. The roles of residues in regions I and II (in models B1 and B2) are supported by earlier mutagenesis results. To test the role of region III residues in granisetron binding, loop B and E residues were mutated, which are assumed to be involved in ligand binding according to models A1 and A2.

**Mutation of Region III Residues and Granisetron Binding to the Mutant Receptors.** The effects of mutations of region III residues on granisetron binding are summarized in Table 1. [<sup>3</sup>H]Granisetron, a 5-HT<sub>3R</sub>-specific competitive antagonist, was bound with high affinity to the receptors expressed in tSA cells ( $K_d = 0.96$  nM). Alanine mutation of H185 resulted in receptors without detectable granisetron binding. An about 5-fold reduction in binding affinity was observed for L184A and H185Y. Alanine mutation of D189 resulted in a dramatic, 22-fold reduction in the affinity of granisetron. Alanine mutations of T186, I187, and Q188 resulted only in minor (1.4–3-fold) changes in granisetron binding. Mutations Y143F and Y153F produced 3.4- and 6.0-fold changes in

the  $K_d$  value of granisetron, similar to what was observed for mutations Y143A and Y153A.

## DISCUSSION

Molecular modeling has been widely used as an important tool to interpret mutation studies of 5-HT<sub>3ARs</sub> (8, 11). Thus far, in the absence of the experimentally determined structure of 5-HT<sub>3Rs</sub>, antagonists were docked to homology models based on ligand-bound AChBP with “lid-shut” binding cavity, even though antagonists seem to stabilize the “lid-open” binding cavities of ionotropic receptors (23). The recently determined structure of the closed nACh receptor-ionophore is a more appropriate template for modeling interactions of antagonists with the extracellular domain of the 5-HT<sub>3</sub> receptor (20). The “lid-open” receptor model raises the possibility that antagonists can enter the binding cavity not only from region I but also from region III. Additionally, models based on the “lid-shut” form of the receptor (8, 11, 30) underestimate the accessible volume of the binding cleft and miss the importance of region III residues. In this study, the “lid-open” homology model was used to dock granisetron into the binding site. It was anticipated that by utilizing a “lid-open” model a more thorough understanding of antagonist binding can be achieved.

**Residues in Binding Loops Interact with Granisetron.** A new homology model of the extracellular domain of 5-HT<sub>3R</sub> was built, and this model was used to dock granisetron into the binding site. The results of the docking studies yielded four different clusters. In models A1 and A2, differing only in orientation, granisetron was found to dock into regions II and III, while in models B1 and B2, granisetron was docked to the earlier identified regions I and II. Previous studies have identified residues in loops A, C, and D (regions I and

II, docked models B1 and B2) playing a critical role in granisetron binding (11, 19, 30). Docking to the "lid-open" model confirmed the previously identified roles of E129, W90, D229, and Y234 in models B1 and B2, which are in similar positions to the docked models based on the "lid-shut" receptor structure (8, 11, 30).

Alanine-scanning mutation studies demonstrated that loop E tyrosines Y141, Y143, and Y153 influence ligand binding (16, 31). Residues Y143 and Y153 in region II are in an interacting distance with granisetron in both models A and B. They can form hydrogen bonds with the carbonyl group in models A1 and A2. To further test the role of the OH groups of these tyrosines, Y143F and Y153F mutations were created. These mutations were found to have similar effects as alanine mutations, suggesting that the reduced affinity might be caused by the lack of the OH group. This finding supports the assumption that above-mentioned residues are involved in hydrogen bonding with granisetron.

In models A1 and A2, granisetron was found to dock into a second position at regions II and III, where loop B residues H185, T186, and D189 are in close proximity of the docked ligands. To confirm the role of these residues, granisetron binding was studied by radioligand binding to receptors mutated in loop B. Mutations of residues within 4 Å of A1 and A2 models L184A, H185A/H185Y, and D189A significantly reduced granisetron binding, supporting our hypothesis of a second binding region (region III). Mutation T186A, near granisetron in our docked models, had only a minor effect on granisetron binding. In accordance with our model, loop B residues not involved in the docked models (I187 and Q188) caused only a slight increase in the  $K_d$  value. In summary, both modeling and mutation data support that, besides W183 (13), other loop B residues (H185 and D189) are also critical in granisetron binding.

**Evaluation of Models A and B.** In this study, both modeling and mutagenesis studies provided evidence that there is region distinct from the formerly defined binding site that influences granisetron binding (region III in Figure 2). The interface between regions II and III is not accessible in studies based on nicotinic agonist-bound AChBP; therefore, these models cannot be found in the docking results of the previous studies (8, 11, 30). Moreover, recently published X-ray structures of AChBP complexed with nicotinic agonists and antagonists show that loop C does not significantly change its orientation upon binding of an antagonist; it opens further upon binding of a peptide antagonist, whereas it wraps around agonists (32). These findings support the assumption that antagonists bind to the "lid-open" receptor.

The important role of region I in granisetron binding has been previously determined. Model B2 is similar to those found in previous studies where granisetron was docked into the "lid-shut" receptor model (8, 11). Models B1 and B2 can explain the experimentally observed essential role of region I and II residues W90, W183, Y234, D229, and E129 in granisetron binding. However, the role of loop E tyrosines located in region III cannot be clarified with models B1 and B2. Further, models B1 and B2 are not able to explain the experimentally observed crucial effects of mutations on region III residues (H185 and D189). H185A and D189A mutations and also mutations W183A, D229A, Y141A, Y153A, and Y234A strongly influenced granisetron binding. These region II and III residues are close to granisetron in

models A1 and A2. Therefore, residues in both the previously identified (regions I and II, models B1 and B2) and in the newly identified (regions II and III, models A1 and A2) regions interact with granisetron in the process of antagonist binding.

The size of granisetron does not permit simultaneous interactions with region I and region III residues. Therefore, because mutations in both regions decrease granisetron binding, it can be assumed that there is a primary site of interaction ("way-in site" of interaction) distinct from the actual high-affinity binding site. The "way-in site" for antagonists might follow this "path" to the binding site, and an initial weaker interaction may help the subsequent high-affinity binding as a final step. In our models, two orientations of granisetron are possible in both binding regions (models A1 and A2 and models B1 and B2; see Figure 3). Dependent upon the orientation of granisetron, either the azobicyclic ring or the indole ring is located in region II. Previous modeling studies and experimental data (8, 11, 30) favor a binding mode similar to model B2. A recent paper by Yan and White (30) indicates that the azobicyclic ring interacts with W90, which is again consistent with model B2. Their data from double-mutant cycling is the strongest data available to indicate orientation. B1 is not consistent with this finding, and therefore, B2 orientation is supported. A shift from B2 to A1 is not likely (although possible) because it would require the molecule to rotate into the final position. Additionally, both the dominant docking frequency and the dominant importance of the W183 residue (cation- $\pi$  interaction with granisetron in model A2) would support an A2 position and orientation. Because B2 and A2 orientations seem to be supported by experimental and molecular modeling data, the binding effects are consistent with a model in which the "way-in site" is at regions I and II in the B2 orientation with a subsequent translation to the A2 position. Binding to the A2 position would preclude closure of the binding site because binding to region III would preclude the lid from "shutting".

## CONCLUSIONS

In this study, we have identified possible binding locations of the specific 5-HT<sub>3</sub>R antagonist granisetron in the "lid-open" binding cavity of the 5-HT<sub>3A</sub>Rs using homology modeling, ligand docking, and radioligand binding of the mutated receptor. Docking studies identified antagonist binding at loops C, B, and D. At this binding site, granisetron hinders the complete closure of the "lid" between regions II and III and precludes the conformational rearrangement of loop B. Mutagenesis studies support these results and have identified critical roles of H185 and D189 in granisetron binding.

## REFERENCES

- Gaddum, J. H., and Picarelli, Z. P. (1957) Two kinds of tryptamine receptor, *Br. J. Pharmacol.* 12, 323–328.
- Maricq, A. V., Peterson, A. S., Brake, A. J., Myers, R. M., and Julius, D. (1991) Primary structure and functional expression of the 5HT<sub>3</sub> receptor, a serotonin-gated ion channel, *Science* 254, 432–437.
- Lummiss, S. C., and Martin, I. L. (1992) Solubilization, purification, and functional reconstitution of 5-hydroxytryptamine<sub>3</sub> receptors from N1E-115 neuroblastoma cells, *Mol. Pharmacol.* 41, 18–23.



4. Green, T., Stauffer, K. A., and Lummis, S. C. (1995) Expression of recombinant homo-oligomeric 5-hydroxytryptamine<sub>3</sub> receptors provides new insights into their maturation and structure, *J. Biol. Chem.* 270, 6056–6061.
5. Morales, M., and Wang, S. D. (2002) Differential composition of 5-hydroxytryptamine<sub>3</sub> receptors synthesized in the rat CNS and peripheral nervous system, *J. Neurosci.* 22, 6732–6741.
6. Niesler, B., Frank, B., Kapeller, J., and Rappold, G. A. (2003) Cloning, physical mapping and expression analysis of the human 5-HT<sub>3</sub> serotonin receptor-like genes HTR3C, HTR3D, and HTR3E, *Gene* 310, 101–111.
7. Brejc, K., van Dijk, W. J., Klaassen, R. V., Schuurmans, M., van der Oost, J., Smit, A. B., and Sixma, T. K. (2001) Crystal structure of an ACh-binding protein reveals the ligand-binding domain of nicotinic receptors, *Nature* 411, 269–276.
8. Maksay, G., Bikádi, Z., and Simonyi, M. (2003) Binding interactions of antagonists with 5-hydroxytryptamine<sub>3A</sub> receptor models, *J. Recept. Signal Transduction Res.* 23, 255–270.
9. Reeves, D. C., Sayed, M. F., Chau, P. L., Price, K. L., and Lummis, S. C. (2003) Prediction of 5-HT<sub>3</sub> receptor agonist-binding residues using homology modeling, *Biophys. J.* 84, 2338–2344.
10. Maksay, G., Simonyi, M., and Bikádi, Z. (2004) Subunit rotation models activation of serotonin 5-HT<sub>3AB</sub> receptors by agonists, *J. Comput.-Aided Mol. Des.* 18, 651–664.
11. Thompson, A. J., Price, K. L., Reeves, D. C., Chan, S. L., Chau, P. L., and Lummis, S. C. (2005) Locating an antagonist in the 5-HT<sub>3</sub> receptor binding site: A modeling and radioligand binding study, *J. Biol. Chem.* 280, 20476–20482.
12. Boess, F. G., Steward, L. J., Steele, J. A., Liu, D., Reid, J., Glencorse, T. A., and Martin, I. L. (1997) Analysis of the ligand binding site of the 5-HT<sub>3</sub> receptor using site directed mutagenesis: Importance of glutamate 106, *Neuropharmacology* 36, 637–647.
13. Spier, A. D., and Lummis, S. C. (2000) The role of tryptophan residues in the 5-Hydroxytryptamine(3) receptor ligand binding domain, *J. Biol. Chem.* 275, 5620–5625.
14. Steward, L. J., Boess, F. G., Steele, J. A., Liu, D., Wong, N., and Martin, I. L. (2000) Importance of phenylalanine 107 in agonist recognition by the 5-hydroxytryptamine(3A) receptor, *Mol. Pharmacol.* 57, 1249–1255.
15. Yan, D., Schulte, M. K., Bloom, K. E., and White, M. M. (1999) Structural features of the ligand-binding domain of the serotonin 5HT<sub>3</sub> receptor, *J. Biol. Chem.* 274, 5537–5541.
16. Venkataraman, P., Joshi, P., Venkatachalan, S. P., Muthalagi, M., Parihar, H. S., Kirschbaum, K. S., and Schulte, M. K. (2002) Functional group interactions of a 5-HT<sub>3R</sub> antagonist, *BMC Biochem.* 3, 16.
17. Venkataraman, P., Venkatachalan, S. P., Joshi, P. R., Muthalagi, M., and Schulte, M. K. (2002) Identification of critical residues in loop E in the 5-HT<sub>3ASR</sub> binding site, *BMC Biochem.* 3, 15.
18. Schreiter, C., Hovius, R., Costioli, M., Pick, H., Kellenberger, S., Schild, L., and Vogel, H. (2003) Characterization of the ligand-binding site of the serotonin 5-HT<sub>3</sub> receptor: The role of glutamate residues 97, 224, and 235, *J. Biol. Chem.* 278, 22709–22716.
19. Suryanarayanan, A., Joshi, P. R., Bikadi, Z., Mani, M., Kulkarni, T. R., Gaines, C., and Schulte, M. K. (2005) Site-directed mutagenesis reveals molecular determinants of differential action of 5-hydroxytryptamine and *meta*-chlorophenylbiguanide at the loop C region of 5-HT<sub>3A</sub> receptor, *Biochemistry* 44, 9140–9149.
20. Celie, P. H. N., Kasharov, I. E., Mordvintsev, D. Y., Hogg, C., van Nierop, P., van Elk, R., van Rossum-Fikkert, S. E., Zhmak, M. N., Bertrand, D., Tsetlin, V., Sixma, T. K., and Smit, A. B. (2005) Crystal structure of nACh receptor homolog AchBP in complex with an  $\alpha$ -conotoxin PNIA variant.
21. Celie, P. H., van Rossum-Fikkert, S. E., van Dijk, W. J., Brejc, K., Smit, A. B., and Sixma, T. K. (2004) Nicotine and carbamylcholine binding to nACh receptors as studied in AchBP crystal structures, *Neuron* 41, 907–914.
22. Unwin, N. (2005) Refined structure of the nicotinic acetylcholine receptor at 4 Å resolution, *J. Mol. Biol.* 346, 967–989.
23. Karlin, A. (2002) Emerging structure of the nicotinic acetylcholine receptors, *Nature Rev.* 3, 102–113.
24. Wu, C. H., Huang, H., Arminski, L., Castro-Alvares, J., Chen, Y., Hu, Z. Z., Ledley, R. S., Lewis, K. C., Mewes, H. W., Orcutt, B. C., Suzek, B. E., Tsugita, A., Vinayaka, C. R., Yeh, L. S. L., Zhang, J., and Barker, W. C. (2002) The protein information resource: An integrated public resource of functional annotation of proteins, *Nucleic Acids Res.* 30, 35–37.
25. Thompson, J. D., Higgins, D. G., and Gibson, T. J. (1994) CLUSTAL W: Improving the sensitivity of progressive multiple sequence alignment through sequence weighting, position-specific gap penalties, and weight matrix choice, *Nucleic Acids Res.* 22, 4673–4680.
26. Xiang, Z., and Honig, B. (2001) Extending the accuracy limits of prediction for side-chain conformations, *J. Mol. Biol.* 311, 421–430.
27. Xiang, Z., Soto, C. S., and Honig, B. (2002) Evaluating conformational free energies: The colony energy and its application to the problem of loop prediction, *Proc. Natl. Acad. Sci. U.S.A.* 99, 7432–7437.
28. Laskowski, R. A., MacArthur, M. W., Moss, D. S., and Thornton, J. M. (1993) PROCHECK: A program to check the stereochemical quality of protein structures, *J. Appl. Crystallogr.* 26, 283–291.
29. Morris, G. M., Goodsell, D. S., Hallaway, R. S., Huey, R., Hart, W. E., Belew, R. K., and Olson, A. J. (1998) Automated docking using a Lamarckian genetic algorithm and empirical binding free energy function, *J. Comput. Chem.* 19, 1639–1662.
30. Yan, D., and White, M. M. (2005) Spatial orientation of the antagonist granisetron in the ligand-binding site of the 5-HT<sub>3</sub> receptor, *Mol. Pharmacol.* 68, 365–371.
31. Price, K. L., and Lummis, S. C. (2004) The role of tyrosine residues in the extracellular domain of the 5-hydroxytryptamine<sub>3</sub> receptor, *J. Biol. Chem.* 279, 23294–23301.
32. Hansen, S. B., Sulzenbacher, G., Huxford, T., Marchot, P., Taylor, P., and Bourne, Y. R. (2005) Structures of *Aplysia* AChBP complexes with nicotinic agonists and antagonists reveal distinctive binding interfaces and conformations, *EMBO J.* 24, 3635–3646.

BI051676F